Tellus (2003), 55A, 419–425
Printed in UK. All rights reserved

TELLUS
ISSN 0280–6495

Gravity wave drag and global angular momentum: geostrophic adjustment processes

By JOSEPH EGGER*, *Meteorologisches Institut, Universität München, Theresienstrasse 37, 80333 Munich, Germany*

(Manuscript received 24 May 2002; in final form 14 March 2003)

ABSTRACT

Current gravity wave drag schemes alter the flow field of a numerical model by changing the velocity. It is argued that this is essentially the situation considered in the theory of geostrophic adjustment. The reduction of velocity at one moment does not necessarily lead to a reduction of the global mean velocity after adjustment in that case. It is best to discuss these processes in terms of angular momentum conservation, so that the initial loss of velocity can be seen as a reduction of the wind term which may be converted into a reduction of the mass term. Observations are used to see if this process can be detected in the angular momentum budget of the atmosphere. The data indeed reveal a rapid positive response of the mass term to the gravity wave drag.

1. Introduction

By now, parameterizations of gravity wave drag are standard ingredients of numerical forecast and general circulation models. This technique is supposed to capture the removal of momentum from the atmosphere due to the breaking of gravity waves induced by orography. These waves are not resolved numerically in these models and therefore their impact must be parameterized. The structure of most gravity wave parameterization schemes can be described as follows (see Kim and Arakawa, 1995 for a review). One assumes first a formulation for the stress τ_s exerted by the gravity waves at the ground. In general

$$\tau_s = \boldsymbol{v}_s C \tag{1.1}$$

where $\boldsymbol{v}_s$ is the horizontal velocity at the surface and C is a complicated function of the terrain, of stability and many other factors (e.g. Gregory et al., 1998; Scinocca and MacFarlane, 2000; Lott and Miller, 1997). In particular, a vertical stress profile τ must be specified with $\tau(h) = \tau_s$ (where h is the resolved topography). In many cases a saturation hypothesis is invoked following Lindzen (1981) which determines the level of wave breaking. The final step is to incorporate the stress in the equations of motion so that

$$\frac{\partial \boldsymbol{v}}{\partial t} = \cdots \rho^{-1} \frac{\partial \tau}{\partial z} \tag{1.2}$$

(ρ is density; $\boldsymbol{v}$, horizontal velocity).

Such parameterizations have been tested extensively using high-resolution models where gravity breaking is calculated explicitly and the resulting gravity wave stress can be compared to that obtained by a parameterization scheme (e.g. Kim and Arakawa, 1995). By and large the results of this intercomparison are encouraging but, as pointed out by Welch et al. (2001), one has to keep in mind that the orography prescribed in these simulations is much simpler than in reality. Durran (1995) demonstrated that wave breaking need not lead to local flow deceleration as assumed in eq. (1.2).

The gravity wave parameterization schemes had some success in reducing model errors (Palmer et al., 1986; Miller et al., 1989). For example, Scinocca and MacFarlane (2000) found a reduction of global root mean square (r.m.s.) mean sea-level pressure

*e-mail: j.egger@LRZ.uni-muenchen.de

and wind errors in boreal winter. On the other hand, Klinker and Sardeshmukh (1992) pointed out that the model error remaining after the implementation of a scheme had the same pattern as that of the parameterized contribution itself. This indicates that the schemes may cause new errors (Welch et al., 2000).

Gravity wave drag need not be linked to orographic excitation. Cumulus convection generates gravity waves which may in turn transport momentum vertically. This process has been incorporated in numerical models as well (e.g. Warner and McIntyre, 2001). In any case, it is clear that the gravity wave drag induces reactions of global scale. For example, Egger and Hoinka (2002) found a response of the global atmospheric angular momentum to the gravity wave torque. However, while elaborate theories of gravity wave breaking have been formulated in a local, non-rotating framework, the corresponding large-scale response of the atmosphere received little attention. It is the angular momentum of the air which is affected by gravity wave drag if eq. (1.2) is used in global models. As will be explained in more detail below, not only the velocity but also the mass distribution responds to the drag. A similar situation has been studied extensively in the theory of geostrophic adjustment, with emphasis on the atmospheric reaction to the removal of momentum (e.g. Blumen, 1972) in a rotating system. Although the theory of geostrophic adjustment per se is not concerned with the effects of gravity wave drag, it will be argued that this theory provides theoretical guidance when applied to this problem. Correspondingly, the atmospheric response to gravity wave drag will first be discussed in terms of geostrophic adjustment (in section 2), with particular emphasis on angular momentum aspects. Then, observations of global angular momentum will be used to test this proposition (section 3).

2. Geostrophic adjustment and angular momentum

Long ago, Rossby (1937; 1938) formulated and solved the prototype problem of geostrophic adjustment. Rossby investigated the atmospheric and oceanic response to rapid removal of momentum. This problem is of immediate concern here [see Blumen (1972) for a concise review]. Rossby considered a shallow water fluid of mean depth H and of infinite

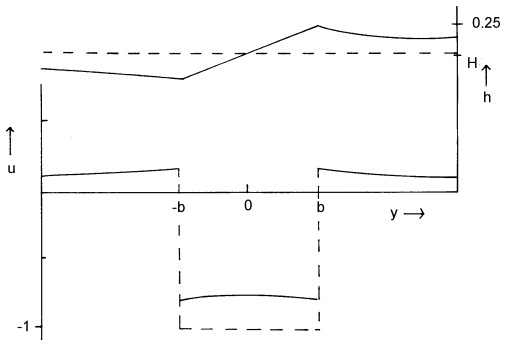

Fig. 1. Asymptotic zonal velocity profile of the shallow water after a unit amount of zonal velocity has been removed instantaneously in the stripe $|y| < b$. Dashed: initial profile; $b/\lambda = 0.2$. Also given is the asymptotic height profile of the free surface. Dashed: unperturbed mean height; units $u_o f_o \lambda / g'$; linear solution.

lateral extent. He stipulated that a certain amount of momentum is impulsively removed from or added to a fluid strip of width $2b$ (see Fig. 1). This is the basic situation of a gravity wave drag acting for a short time. Rossby analyzed the asymptotic steady-state response of the fluid. Cahn (1945) solved the corresponding linear initial value problem. The height of the shallow water adjusts near the strip $|y| < b$ such that the sloping surface of the fluid balances geostrophically the resulting zonal flows, while inertia–gravity waves propagate meridionally. Zonal propagation is excluded in this case because the initial perturbation depends on y only. The main point of interest here is the angular momentum budget of this solution. The first thing to note is that the meridionally averaged mean zonal wind perturbation vanishes after the inertia–gravity waves have left the domain. To see this we have to calculate the vorticity distribution after removal of velocity u_o in the strip $|y| < b$. Obviously, the initial distribution of vorticity is

$$\zeta_i = \delta[(y+b)/b] - \delta[(y-b)/b] u_o / b \qquad (2.1)$$

[i denotes initial; $\delta(y)$ is the delta function]. The resulting streamfunction is, after linear adjustment (see Blumen, 1972),

$$\psi(y) = -\frac{\lambda}{2} \int_{-\infty}^{\infty} \zeta_i(\varepsilon) \exp(-|y-\varepsilon|/\lambda)\, d\varepsilon \qquad (2.2)$$

where $\lambda = (g'H)^{1/2} f_0^{-1}$ is the Rossby radius of deformation (g' is reduced gravity). Thus, the steady-state zonal wind profile becomes, with $u = -\,\mathrm{d}\psi/\mathrm{d}y$,

$$u = \begin{cases} \frac{1}{2} u_o \{\exp[(y+b)/\lambda] - \exp[(y-b)/\lambda]\} & \text{for } y < b \\ \frac{1}{2} u_o \{-\exp[-(y+b)/\lambda] - \exp[(y-b)/\lambda]\} & \text{for } -b < y < b \\ \frac{1}{2} u_o \{-\exp[-(y+b)/\lambda] + \exp[-(y-b)/\lambda]\} & \text{for } y > b \end{cases} \tag{2.3}$$

where $u_o > 0$. The flow is easterly within the strip and comes closer to $-u_o$ the smaller b/λ becomes. Westerlies are found outside the strip because there ψ decreases with increasing y (Fig. 1), so that

$$\bar{u} = \int_{-s}^{s} u \,\mathrm{d}y = -\psi(s) + \psi(-s) \sim 0 \tag{2.4}$$

for $s \gg b$, $s > \lambda$. This means that the removal of momentum due to a gravity wave drag parameterization does not lead to a final reduction of zonal flow velocity when averaged over a wider strip of width 2λ, say. This is rather surprising. After all, momentum has been removed initially but eq. (2.4) tells us that there is no total loss of mean velocity. This suggests in turn that removal of momentum by a gravity wave drag scheme need not lead to a reduction of the mean flow velocity. This puzzle can be resolved, of course, by looking at the first equation of motion, which is

$$\frac{\partial u}{\partial t} - f_o v = 0 \tag{2.5}$$

in the context of linear theory. In eq. (2.5), v is the meridional velocity and $f_o = 2\Omega \sin\varphi_o$ is the Coriolis parameter ($\Omega = 2\pi/\mathrm{d}$; φ_o is latitude, a constant). With

$$v = \frac{\partial \eta}{\partial t} \tag{2.6}$$

it follows that

$$\frac{\partial}{\partial t}(u - f_o \eta) = 0 \tag{2.7}$$

where η is the meridional deviation of the position of a particle from its initial state. The variable

$$m = u - f_o \eta \tag{2.8}$$

can be seen as a specific angular momentum of the f-plane flow. The specific axial angular momentum

$$m_s = (u + \Omega a \cos\varphi) a \cos\varphi \tag{2.9}$$

of spherical shallow water flow can be shown to reduce to eq. (2.8) if expanded near the latitude φ_o (e.g. Egger, 2001). Initially $m = -u_o$ for $|y| < b$, so that we have $\bar{m} = -u_0 2b$. Thus, if $\bar{u} = 0$ later on according to eq. (2.4), it follows that $\bar{\eta} = 2 f_o^{-1} u_o 2b$ from eq. (2.7).

There is a mean northward shift of the particles in the area of momentum removal. This shift simply reflects the buildup of a ridge at $y = b$ and of a trough at $y = -b$ (Fig. 1). The related pressure gradient has to balance the zonal wind [eq. (2.3)]. In other words the flow profile of eq. (2.3) indicates that eastward acceleration has been acting everywhere, which calls for a northward shift of mass. All in all, the theory of geostrophic adjustment predicts that all the momentum removed by the gravity wave drag scheme is converted into meridional mass shifts which conserve angular momentum. In principle, the inertia–gravity waves could also transport angular momentum, but as can be seen from eqs. (2.5) and (2.6) that is impossible owing to the leading order for linear surface waves. If $m = 0$ initially for $|y| > b$, $m = 0$ for all time. One may go to second order, where the inertia–gravity waves contain and transport angular momentum. However, such effects may be disregarded here as being small. The time scale of adjustment is f_o^{-1}. Of course, models of higher dimension including stratification should be considered as well, but, as Blumen (1972) points out, the results obtained with such models are "in essential agreement" with the fundamental principles discussed above.

Here, we wish to apply these ideas to the gravity wave drag problem by analysing the response of global atmospheric angular momentum to this drag. In particular, we want to find out if the conversion of angular momentum from the winds to meridional shifts of particles as predicted by the theory of geostrophic adjustment can be observed.

The global angular momentum

$$\boldsymbol{M} = \int_V \rho \boldsymbol{r} x (\boldsymbol{v} + \boldsymbol{\Omega} x \boldsymbol{r}) \,\mathrm{d}V = \boldsymbol{M}_w + \boldsymbol{M}_m \tag{2.10}$$

(where V is the volume of the atmosphere, $\boldsymbol{r}$ position vector, and $\boldsymbol{\Omega}$ the earth's rotation vector) is a vector. Let us introduce a coordinate system with origin at

the center of the earth where the z-axis coincides with the earth's rotation axis and the $x(y)$-axis is embedded in the equatorial plane pointing towards $\varphi = 0, \lambda = 0$ ($\varphi = 0, \lambda = \pi/2$) where standard spherical coordinates are used. The two equatorial components are M_x and M_y, and M_z is the axial component. The first term on the right of eq. (2.10) is the so-called wind term $\boldsymbol{M}_{\mathrm{w}}$, while the second one is the mass term $\boldsymbol{M}_{\mathrm{m}}$. Obviously, the wind term corresponds with the zonal velocity u in eq. (2.7), while the mass term is represented by the term $-f_{\mathrm{o}}\eta$.

The global angular momentum is exposed to mountain torque $\boldsymbol{T}_{\mathrm{o}}$, to friction torque $\boldsymbol{T}_{\mathrm{f}}$, to torques linked to the non-spherical shape of the earth (e.g. Bell, 1994; Egger and Hoinka, 2002) and to a torque $\boldsymbol{T}_{\mathrm{g}}$ due to the gravity waves. In principle, $\boldsymbol{T}_{\mathrm{g}}$ is part of $\boldsymbol{T}_{\mathrm{o}}$ because the torque exerted by orography includes that due to topographically induced gravity waves. In practice, there is a difference, of course, in that the orographic torques available from global analyses include only those torques exerted by motions resolved in the analysis scheme. They do not include gravity wave effects. In other words, we do have observations of $\boldsymbol{T}_{\mathrm{o}}$ with respect to larger scales but not at the level of gravity waves. Available gravity wave torques are estimated on the basis of the parameterization schemes mentioned above.

The gravity wave drag parameterization acts on the wind term only. The wind speed tendency is altered instantaneously [see eq. (1.2)] during a gravity wave drag event. If our analogy to the geostrophic adjustment problem is correct a conversion from the wind term to the mass term occurs after the action of the drag. This prediction can be tested by investigating the response of mass and wind terms to the gravity wave drag using observations.

One may argue that it is only the axial angular component M_z which is represented reasonably well by the f-plane flow equations (Egger, 2001) discussed above, so that M_x and M_y need not be affected by geostrophic adjustment. However, the redistribution of mass typical of geostrophic adjustment must affect all three components of the mass term in eq. (2.10). Although it is certainly true that the changes in $M_{\mathrm{m}x}$, $M_{\mathrm{m}y}$ during geostrophic adjustment differ from those in M_z, it is also obvious that the conversion from wind to mass terms must also be observable for the equatorial components.

The analysis of the role of $\boldsymbol{T}_{\mathrm{g}}$ in the angular momentum budget relies on the ERA data for the years 1979–1992 (European center of medium range forecast ReAnalysis project; Gibson et al., 1997). The data are available four times a day but smoothed so that diurnal variations are not resolved. The wind terms contain a large diurnal signal which must be removed to see more clearly the structure of the covariance functions. Wind and density are available at 31 levels with spectral resolution T106. More details on the data set are found in Egger and Hoinka (2002). We will mainly look at covariance functions $C(a;\ b \mid \tau) = E[a(t)\ b(t+\tau)]$ of variables a and b, where E is the expectation and τ the lag.

It must be stressed that the parameterizations of gravity wave drag are fraught with many incertainties. It is by no means certain that gravity waves break in the atmosphere at the location and at the time indicated by a scheme. For example, Benoit et al. (2002) used a high-resolution model to predict air flow over the Alps during the Mesoscale Alpine Project. Gravity waves were resolved by this model and predicted to break at several occasions. However, research aircraft flying to these locations were not able to find such events. Of course, parameterizations of such processes are less reliable than direct simulations. They may be correct at best in a statistical sense. This invites the question why we would expect to see any atmospheric reaction to events which are predicted but presumably rarely occur the way they are predicted. We have to keep in mind, however, that the analysis cycle of the ERA project blends observations and model results. The parameterization scheme operates in the forecast model of ECMWF and the model atmosphere responds to the reduction of velocity. Assume now that this happens in an area with little data coverage such as the stratosphere or above the plateau of Tibet. The analysis scheme gives a large weight to the predictions of the model in such areas and accepts the model response as observations even if the prediction of wave breaking was incorrect. If, on the other hand, data coverage is good the analysis scheme may reject the model response and no reaction to the drag will be found in the data. On average, however, we feel confident that the geostrophic adjustment process outlined above must be reflected in the ERA data.

3. Results

The typical duration of gravity wave events is an important parameter. It is assumed in the geostrophic adjustment problem that the removal of momentum occurs instantaneously. The duration of gravity wave breaking events in the atmosphere is not known. We

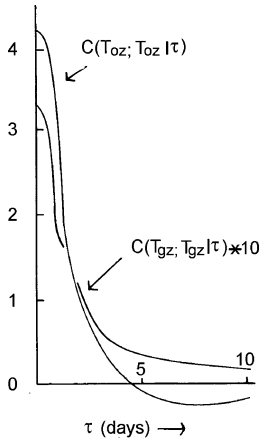

Fig. 2. Autocovariance function $C(T_{gz}; T_{gz} \mid \tau)$ of axial gravity wave torque T_{gz} and autocovariance $C(T_{oz}; T_{oz} \mid \tau)$ of axial mountain torque T_{oz} for lags $\tau \leq 10$ d in units of 10^{38} kg^2 m^4 s^{-4}.

can, however, evaluate the typical time scale of such events as resulting from the parameterization scheme by looking at the autocovariance functions of the drag. The autocovariance function $C(T_{gz}; T_{gz} \mid \tau)$ of the axial drag T_{gz} is displayed in Fig. 2 together with the autocovariance of the resolved mountain torque T_{oz}. The variance of T_{gz} is, of course, smaller than that of T_{oz}. Both covariances decay rather fast for small lags. However, while the first zerocrossing of $C(T_{oz}; T_{oz} \mid \tau)$ occurs for $\tau \sim 4$ d, there is a long positive tail of the autocovariance function of T_{gz}. The same is true for T_{gy}, T_{oy} (Fig. 3) and T_{gx}, T_{ox} (not shown).

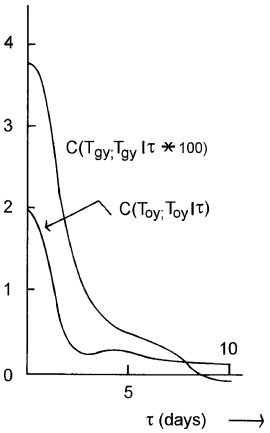

Fig. 3. Autocovariance function $C(T_{gy}; T_{gy} \mid \tau)$ of equatorial gravity wave torque T_{gy} and of mountain torque T_{oy} for lags $\tau \leq 10$ (d) in units of 10^{39} kg^2 m^4 s^{-4}.

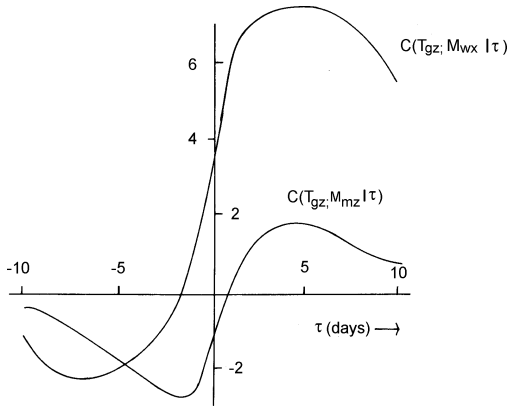

Fig. 4. Crosscovariance functions $C(T_{gz}; M_{wz} \mid \tau)$ and $C(T_{gz}; M_{mz} \mid \tau)$ of the axial gravity wave torque T_{gz} and the axial wind and mass terms for lags $|\tau| \leq 10$ d in units of 10^{42} kg^2 m^4 s^{-3}.

It follows from Figs. 2 and 3 that gravity wave drag events tend to be rather longlived. In particular, they last longer than mountain torque events. This result is presumably unrealistic. Note that all autocovariances are quite small for lags $\tau > 8$ days, say. Because of this, we will present crosscovariances only for lags less than 10 days in what follows.

The crosscovariance functions of T_{gz} and the wind and mass terms are shown in Fig. 4. The correlation of T_{gz} and M_{wz} is positive, as one would expect. Moreover, M_w increases for $0 \leq \tau \leq 3$ d in response to the torque with its long memory. The correlation of T_{gz} with the mass term is negative. The reasons for this result are not clear. However, M_{mz} increases rapidly for $0 \leq \tau \leq 3$ d, in agreement with the ideas of geostrophic adjustment. The gravity wave drag affects M_{wz} directly [see eq. (1.2)] but not M_{mz}, in rough agreement with the idea of geostrophic adjustment. There is, however, no indication that the gain of the wind term due to T_{gz} is completely converted to M_{mz}, as suggested by the simple example in Fig. 1.

The correlation of T_{gx} and M_{wx} is negative (Fig. 5), while that of T_{gz} and M_{wz} is positive (Fig. 4). It is likely that this difference is due to the earth's rotation. The equations for M_x, M_y are linked by rotational terms (e.g. Bell, 1994) while that for M_z does not contain such a term. Correspondingly, the response of M_x, M_y to torques is more complicated than that of M_z (Egger and Hoinka, 2002). The increase of the mass term M_{mx} is almost dramatic for $0 \leq \tau \leq 10$ d. This indicates strongly that there is a conversion from the wind term. The response of the mass term M_{my} is weaker than that

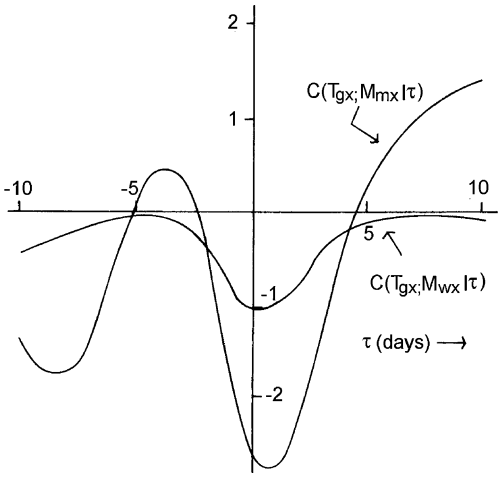

Fig. 5. Crosscovariance functions of the equatorial gravity wave torque (a) T_{gx} and (b) T_{gy} with the respective wind and mass terms for lags $|\tau| \leq 10$ d in units of 10^{42} kg^2 m^4 s^{-3}.

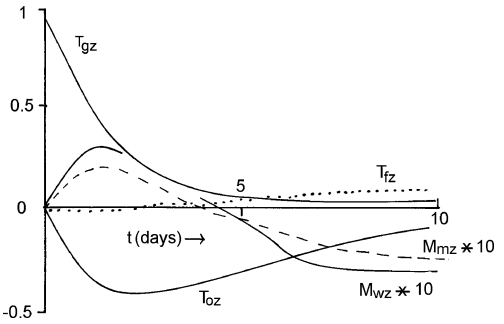

Fig. 6. Response of angular momentum terms and torques to a unit gravity wave torque prescribed at $t = 0$ according to the linear regressive model (3.1). Torques in units of kg m^2 s^{-2}, angular momenta in units of 10^6 kg m^2 s^{-1}.

of M_{mx} (not shown). The reason for this difference of responses is not known. It is, however, important to keep in mind that the mass and wind terms are uncorrelated for all three components (Egger and Hoinka, 2002). Therefore, the parallel increases of mass and wind terms in Figs. 4 and 5 do not reflect any 'automatic' linkage of both terms.

Further insight into the dynamics of the gravity wave drag can be obtained by constructing a regressive model of first order

$$\boldsymbol{x}_{n+1} = \boldsymbol{A} \cdot \boldsymbol{x}_n \tag{3.1}$$

for the data vector $\boldsymbol{x}_n = (M_{wz}, M_{mz}, T_{gz}, T_{oz}, T_{fz})$ where the coefficients of the matrix $\boldsymbol{A}$ involve information on the covariances between the components of $\boldsymbol{x}$ with lags 0 and Dt (see, for example, von Storch and Zwiers, 1999, for details) and $t = n$Dt is time with sampling interval Dt = 6 h. Although eq. (3.1) contains less information than the foregoing figures, we can extract form eq. (3.1) a typical reaction of the mass and wind terms to a unit gravity wave torque. In other words, we specify $T_{gz} = 1$ kg m^2 s^{-2}, M_{mz}, M_{wz}, T_{oz}, $T_{fz} = 0$ at $n = 0$ and integrate eq. (3.1) forward in time. The result is presented in Fig. 6. Both the wind and mass terms increase during the first two days, although T_{gz} acts on M_{wz} only in the analysis scheme. Thus eq. (3.1) represents the conversion from the wind term to the mass term. The gravity wave torque itself is decaying exponentially. There is no link between T_g and the friction torque. There is, however, a pronounced initial decrease of the mountain torque. As one might expect, T_{gz} and T_{oz} are linked statistically.

All in all, Fig. 6 reinforces the conclusions drawn above. The action of gravity wave torques immediately affects the mass term because the adjustment process is operating all the time.

4. Conclusion and discussion

This note proposes that the reaction of the large-scale flow to gravity wave torques can be understood at least partially in terms of a geostrophic adjustment process. Activation of the gravity wave drag scheme leads to a local change of the horizontal velocity. The theory of geostrophic adjustment predicts that the mass distribution will react to such a change to establish geostrophic equilibrium in the domain of velocity changes. The wind and mass terms of the global angular momentum are gross indicators of such processes. The gravity wave drag affects the wind term, but reactions of the mass term must follow in support of our hypothesis. This support has been found by looking at the cross-covariance functions of angular momenta and the gravity wave torque. Although the torque acts on the wind terms only, the data show clearly that there is a rapid conversion to the mass terms. All this means that the impact of gravity wave drag should not be seen only in terms of velocity reduction.

One may argue that geostrophic adjustment is not a meaningful concept in the equatorial belt. It should be kept in mind, however, that the geostrophic adjustment process has been chosen here as a well understood example of how the atmosphere reacts to imposed changes of the wind. The details of this

process are not really relevant in our context. What matters is the basic message that changes of the wind must be seen as changes of the wind term, which may induce a response of the mass term within the framework of global angular momentum conservation. These reactions occur in the Tropics as well as at mid-latitudes. They can therefore be detected both in the equatorial and the axial components of global angular momentum.

It must be kept in mind that there is no observational evidence that the gravity wave drag events forecast by the model of ECMWF occur indeed at the location and time as predicted. Their impact on the mass field is, however, predicted as well. The data analyzed here reflect a blend of observations and predictions. It is impossible to disentangle the effects of gravity wave breaking as occurring in the atmosphere and those occurring in the forecast model only.

REFERENCES

Bell, M. 1994. Oscillations in the equatorial components of the atmosphere's angular momentum and torques on the earth's bulge. *Q. J. R. Meteorol. Soc*. **120**, 195–213.

Benoit, R., Schär, C., Binder, P., Chamberland, S., Davies, H. C. and co-authors. 2002. The real-time ultrafine scale forecast support during the special observing period of the MAP. *Bull. Am. Meteorol. Soc*. **83**, 88–109.

Blumen, W. 1972. Geostrophic adjustment. *Rev. Geophys. Sp. Phys*. **10**, 485–528.

Cahn, A. 1945. An investigation of the free oscillations of a simple current system. *J. Meteorol*. **2**, 113–119.

Durran, D. 1995. Do breaking mountain waves decelerate the local mean flow? *J. Atmos. Sci.* **52**, 4010–4032.

Egger, J. 2001. Angular momentum of β-plane flows. *J. Atmos. Sci.* **58**, 2502–2508.

Egger, J. and Hoinka, K.-P. 2002. Covariance analysis of the global atmospheric axial angular momentum budget. *Mon. Wea. Rev.* **130**, 1063–1070.

Gibson, R., Kållberg, P., Uppala, S., Hernandez, A., Nomura, A. and Serrano, E. 1997. ERA description. *ERA Reanalysis Proj. Rep. Ser.* Vol. 1, 68 pp. [Available from ECMWF, Shinfield Park, Reading RGZ9AX, UK].

Gregory, D., Shutts, G. and Mitchell, J. 1998. A new gravity-wave-drag scheme incorporating anisotropic orography and low-level wave breaking: impact upon the climate of the UK Meteorological Office Unified Model. *Q. J. R. Meteorol. Soc.* **124**, 463–493.

Kim, Y.-J. and Arakawa, A. 1995. Improvement of orographic gravity wave parameterization using a mesoscale gravity wave model. *J. Atmos. Sci.* **52**, 1875–1902.

Klinker, E. and Sardeshmukh, P. 1992. The diagnosis of mechanical dissipation in the atmosphere from large-scale balance requirements. *J. Atmos. Sci.* **49**, 608–627.

Lindzen, R. 1981. Turbulence and stress owing to gravity wave and tidal breakdown. *J. Geophys. Res.* **86**, 9707–9714.

Lott, F. and Miller, M. 1997. A new sub-grid-scale orographic drag parameterization: its formulation and testing. *Q. J. R. Meteorol. Soc.* **123**, 101–127.

Miller, M., Palmer, T. and Swinbank, R. 1989. Parameterization and influence of subgrid-scale orography in general circulation and numerical weather prediction models. *Meteorol. Atmos. Phys.* **40**, 84–109.

Palmer, T. Shutts, G. and Swinbank, R. 1986. Allevation of a systematic westerly bias in general circulation and numerical weather prediction models through an orographic gravity wave parameterization. *Q. J. R. Meteorol. Soc*. **112**, 1001–1039.

Rossby, C.-G. 1937. On the neutral adjustment of pressure and velocity distributions in certain simple current systems. *1. J. Marine. Res.* **1**, 15–25.

Rossby, C.-G. 1938. On the neutral adjustment of pressure and velocity distributions in certain simple current systems. *2. J. Marine. Res.* **1**, 239–263.

Scinocca, J. and McFarlane, A. 2000. The parameterization of drag induced by stratified flow over anisotropic orography. *Q. J. R. Meteorol. Soc.* **126**, 2253–2293.

von Storch, H. and Zwiers, F. 1999. Statistical analysis in climate research. Cambridge University, Press, Cambridge. 484 pp.

Warner, C. and McIntyre, M. 2001. An ultrasimple spectral parameterization of nonorographic gravity waves. *J. Atmos. Sci.* **58**, 1837–1857.

Welch, W., Smolarkiewicz, P., Rotunno, R. and Boville, B. 2001. The large-scale effects of flow over periodic mesoscale topography. *J. Atmos. Sci.* **58**, 1477–1492.